Integral (VOCs, CO_2, mercaptans and H_2S) photosynthetic biogas upgrading using innovative biogas and digestate supply strategies

Mariana Franco-Morgado[1, 2], Alma Toledo-Cervantes[3], Armando González-Sánchez[2], Raquel Lebrero[1], Raúl Muñoz[1]*

1. Department of Chemical Engineering and Environmental Technology, University of Valladolid, C/Dr. Mergelina s/n., Valladolid 47011, Spain.

2. Instituto de Ingeniería, Universidad Nacional Autónoma de México, Circuito Escolar, Ciudad Universitaria, C.P. 04510. México City, México.

3. Departamento de Ingeniería Química, CUCEI-Universidad de Guadalajara, Blvd. M. García Barragán 1451, C.P. 44430, Guadalajara, Jalisco, México.

*Author for correspondence: mutora@iq.uva.es

Abstract

The performance of a pilot high rate algal pond (HRAP) interconnected with a biogas absorption column during the simultaneous upgrading of biogas and treatment of digestate was evaluated under two innovative biogas and nutrient supply strategies. Process operation with biogas supply during the night at a liquid recirculation/biogas ratio of 0.5 to prevent N_2 and O_2 stripping resulted in a biomethane complying with most international regulations for injection into natural gas grids (99.1 ± 1% CH_4, 0.5 ± 0.2% CO_2, 0.6 ± 0.5% N_2 and 0.07 ± 0.08% O_2). The potential of this technology to remove methyl mercaptan (MeSH), toluene and hexane from biogas (typically present at trace levels) was assessed, for the first time, with removal efficiencies under steady-state correlating with pollutant hydrophobicity (7 ± 7% for hexane, 66 ± 4% for MeSH and 98 ± 1% for toluene). Finally, the supply of

digestate during the dark period shifted both microalgae population structure and biomass composition in the HRAP without a significant impact on biomethane quality. Overall, the removal of nitrogen and phosphorous from digestate in the HRAP was almost complete (96-99%) regardless of the nutrient supply strategy.

Keywords: Algal-bacterial symbiosis; Biomethane; Microalgae composition; Photobioreactor; VOCs abatement.

1. Introduction

Biogas produced from the anaerobic digestion of organic solid wastes and wastewaters represent a renewable energy source that can partially alleviate the dependence on conventional fossil fuels. The composition of biogas is mainly governed by the oxidation/reduction state of the organic matter digested, environmental conditions and anaerobic digester configuration. Typically, biogas is composed of methane (CH_4) 40-75%, carbon dioxide (CO_2) 25-60%, hydrogen sulfide (H_2S) 0.005-2%, nitrogen (N_2) < 2%, carbon monoxide (CO) < 0.6%, ammonia (NH_3) < 1%, oxygen (O_2) 0-1%, water (H_2O) 5-10% and trace levels of mercaptans, linear hydrocarbons and toluene (C_7H_8) [1,2]. The final use of biogas (*e*.g. heat and/or electricity generation, injection into natural gas grids, vehicle fuel) determines the level of upgrading required to meet the ultimate quality specifications [3]. For instance, the injection of biogas into natural gas grids (*i.e.* biomethane) is nowadays the biogas standard with the strictest composition requirements (CH_4 > 95%, CO_2 < 2%, O_2 < 0.2-0.5%, H_2S< 5 mg m^{-3}, NH_3 < 3-20 mg m^{-3}, mercaptans < 5-10 mg m^{-3}, aromatic compounds <1 mg m^{-3}, BTX < 50-500 ppm according to European regulations) [3,4].

Several physical-chemical technologies such as chemical/organic/water scrubbing, pressure swing adsorption, and membrane separation are commercially available to upgrade biogas to biomethane. However, the high investment and operating costs of physical-chemical technologies still limit the economic viability of biomethane [3]. In this context, algal-bacterial photobioreactors have emerged as a promising technology for the simultaneous removal of the main biogas contaminants (*i.e.* CO_2 and H_2S) [5]. Photosynthetic biogas upgrading is based on the simultaneous fixation of CO_2 by microalgae and oxidation of H_2S

to SO_4^{2-} by sulfur-oxidizing bacteria using the O_2 photosynthetically produced. It is important to highlight that the environmental and economic feasibility of algal-bacterial photobioreactors devoted to biogas upgrading has been recently enhanced by using the digestate from the anaerobic digester as a water and nutrient source to support microbial growth [6,7]. The photobioreactor configuration typically involves a High Rate Algal Pond (HRAP) interconnected to a biogas Absorption Column (AC) via recirculation of the algal cultivation broth. High CO_2 and H_2S removal efficiencies (97-99% and 98-100%, respectively) have been reported using this process configuration, which allows recovering a biomethane complying with most European regulations for injection into natural gas grids [7].

Among the main bottlenecks of this innovative technology is the contamination of biomethane with the O_2 stripped-out from the recirculating cultivation broth in the absorption column. Microalgal photosynthesis in the HRAP is the main responsible for the dissolved oxygen that prevents complying with the strict O_2 levels imposed by biomethane standards [12–14]. In this regard, different strategies have been implemented with limited success to decrease the O_2 content in the upgraded biogas such as the use of co-current flow operation in the absorption column, a decrease in the recirculation liquid/biogas ratio (L/G) or the dosing of the digestate directly into the absorption column [7,12–14]. Biogas supply during the dark period (when dissolved oxygen concentrations are low as a result of the null photosynthetic activity and active microalgal respiration) represents a promising and easy strategy to implement for minimizing oxygen stripping to biomethane.

On the other hand, little is known about the potential of algal-bacterial photobioreactors to remove trace contaminants from biogas such as volatile organic compounds (VOCs) and

mercaptans. Typically, VOCs biotreatment can be effectively performed in bacterial or fungal biofilters, where different elimination capacities can be reached depending on the solubility and concentration of the target VOCs, [8,9]. In this context, Borde et al., [10] reported the potential of algal-bacterial cultures for the biodegradation of salicylate, phenol, and phenanthrene with removal efficiencies >85%. Similarly, Anbalagan et al., [11] demonstrated the effective removal of CO_2 and toluene (89 %) from flue-gas by culturing an indigenous microalgal-bacterial consortium in a tubular photobioreactor.

At this point, it is worth to highlight that during the upgrading of gas streams using microalgal-bacterial cultures, all microorganisms involved are subjected to dynamic changes depending on the operational conditions, the time of exposure to gas contaminants and nutrients supply [15]. Therefore, the ad-hoc control of microalgae biomass composition during the photosynthetic biogas upgrading can enhance the economic sustainability of the process by producing a biomass feedstock with a tailored valorization potential. In this context, Kleerebezem and co-workers reported a significant increase in the carbohydrate content of microalgae when nutrients were supplied during the dark period, which promoted the enrichment of microalgae capable of growing based on the intracellular polyglucose accumulated during the illuminated period in excess of CO_2 [16].

This work aimed at evaluating, for the first time, the abatement of VOCs and mercaptans from biogas in a pilot HRAP interconnected to a biogas absorption column via an external recirculation broth at high alkalinity. Furthermore, the potential of innovative operational strategies such as the supply during the night of biogas (to minimize O_2 stripping to biomethane) and digestate (to promote the accumulation of high-energy storage compounds in the microalgae biomass) was assessed.

2. Materials and methods

2.1 Experimental set-up and operational conditions

The experimental set-up consisted of a 180 L HRAP (1.2 m^2 of illuminated area) interconnected in series to a 10 L conical settler and to a 2.2 L absorption column (170 cm height and 4.4 cm internal diameter) via an external recirculation of the algal-bacterial cultivation broth (Figure 1). The HRAP was continuously agitated at 20 cm s^{-1} by a six blade paddle wheel and illuminated at 1838 ± 451 μmol m^{-2} s^{-1} by six high intensity LED PCBs (Phillips SA, Spain) using 12:12 h light:dark cycles. The HRAP was inoculated with an algal-bacterial consortium from a previous experiment [14] and operated with digestate (obtained from the wastewater treatment plant of Valladolid) as nutrient source. Digestate, with a final composition of Chemical Oxygen Demand (COD) 949 ± 277 mg L^{-1}, Inorganic Carbon (IC) 1430 ± 90 mg L^{-1}, Total Nitrogen (TN) 1345 ± 95 mg L^{-1}, Total Phosphorous (TP) 36 ± 6 mg L^{-1} and a pH of 7.6 ± 0.3, was supplied to the HRAP at 1 L d^{-1}. Synthetic biogas (Abello Linde; Spain) was sparged at 60.5 ± 3.6 L d^{-1} through a stainless steel gas diffuser (pore size of 2μm) located at the bottom of the biogas AC, and operated at a liquid recirculation/ biogas ratio (L/G) of 0.5 using the biomass-free supernatant from the settler (Figure 1). The effluent from the HRAP (doped with a Chemifloc CV-300 flocculant solution) overflowed to the settler, where the algal-bacterial biomass harvested was drawn to set a constant biomass productivity of 15 g m^{-2} d^{-1} throughout the experiment [17]. The excess of the biomass settled was returned to the HRAP to avoid the development of anaerobic conditions due to biomass accumulation. Additionally, tap water was constantly

added to the HRAP in order to compensate for water evaporation using a zero effluent strategy as reported elsewhere [7].

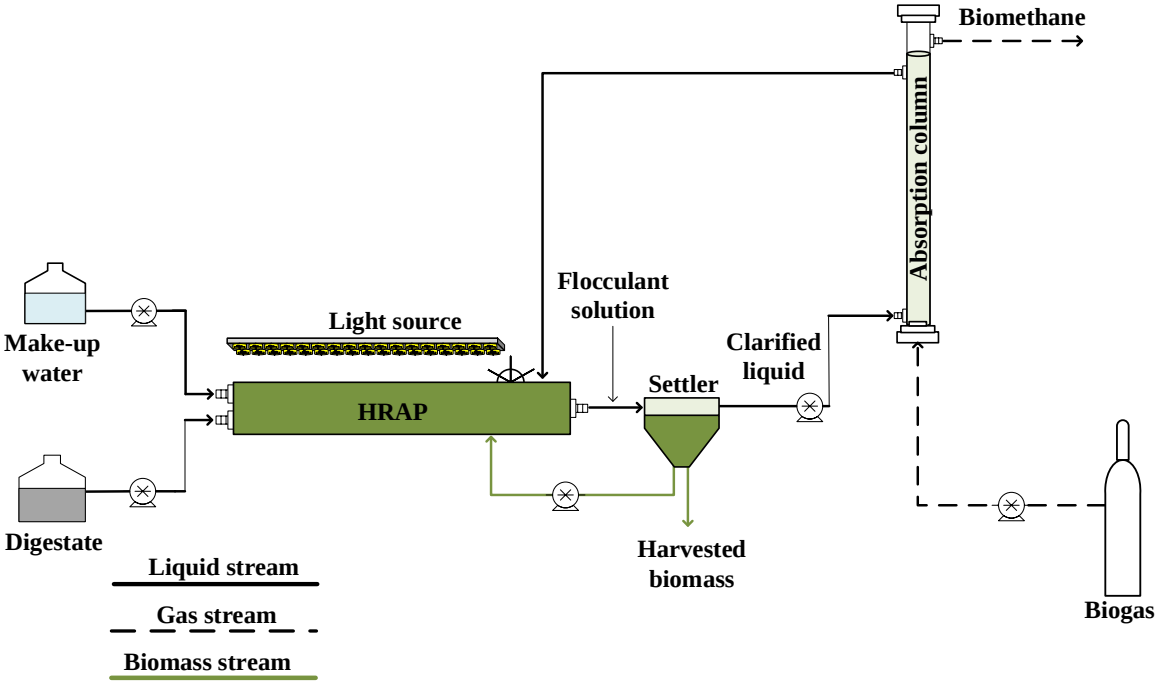

Figure 1. Experimental set-up for the integral photosynthetic biogas upgrading.

The experimental system was previously operated for 220 days with a similar centrate and biogas supply during the illuminated period under multiple operational conditions, which promoted the establishment of an unialgal culture of *Mychonastes homosphaera (Skuja) Kalina & Puncochárová* [14]. Then, the new operational conditions here reported were set and therefore an acclimation phase of 2 weeks was required to stabilize nutrient removal and biomass concentration prior to the beginning of this experiment. Stage I (days 0-30) was only devoted to assessing the feasibility of photosynthetic biogas upgrading in algal-bacterial photobioreactors with biogas injection ($CH_4/CO_2/H_2S$ 70%/29.5%/0.5%) during the dark period (in order to prevent O_2 stripping to the biomethane) and digestate supplementation during the illuminated period (Table 1). The potential of the HRAP-AC to

140 remove methyl mercaptan (MeSH; 21.2 mg m^{-3}), toluene (Tol; 12.2 mg m^{-3}) and hexane
141 (Hex; 47.4 mg m^{-3}) from biogas was evaluated during stage II (days 31-120), which was
142 carried out under biogas injection during the dark period and digestate supplementation
143 during the illuminated period. Finally, the influence of digestate supplementation during the
144 dark period (in order to promote the growth of photosynthetic microorganisms capable of
145 accumulating energy storage compounds during the illuminated period) was assessed in
146 stage III (days 121-171), which was also conducted with the injection during the dark
147 period of the biogas supplemented with MeSH, Tol and Hex (Table 1). This study
148 constitutes, to the best of our knowledge, the first attempt to evaluate the VOCs and
149 Volatile Sulphur Compounds (VSCs) abatement potential of this technology and the
150 influence of biogas and digestate supplementation during the dark periods in HRAPs.
151
152 Aliquots of 100 mL of liquid samples were periodically taken from the digestate and HRAP
153 cultivation broth in order to monitor the total suspended solids (TSS) concentration, IC,
154 TN, ammonium ($N\text{-}NH_4^+$), nitrite ($N\text{-}NO_2^-$), nitrate ($N\text{-}NO_3^-$), sulphate ($S\text{-}SO_4^{2-}$), phosphate
155 ($P\text{-}PO_4^{3-}$), TP and COD concentrations during the three operational stages. pH, temperature
156 and dissolved oxygen (DO) were also measured in the cultivation broth of the HRAP
157 during the illuminated and dark periods. In addition, samples of the cultivation broth were
158 drawn, under steady-state, to monitor the structure of microalgae population and the
159 macromolecular composition of the algal-bacterial biomass (the latter was monitored at the
160 end of the illuminated and dark periods). Gas samples from the inlet and outlet of the
161 absorption column were taken twice a week, by GC-TCD and SPME-GC-FID, to determine
162 the gas concentrations of CH_4, CO_2, H_2S, O_2, N_2, MeSH, toluene, and hexane.

Table 1. Operational conditions evaluated in the experimental HRAP-AC system

Stage	Digestate feeding	Synthetic biogas composition*
I	Illuminated period	CH_4 (70%), CO_2 (29.5%) and H_2S (0.5%)
II	Illuminated period	CH_4 (70%), CO_2 (29.5%), H_2S (0.5%), MeSH (21.2 mg m^{-3}), Toluene (12.2 mg m^{-3}), Hexane (47.4 mg m^{-3})
III	Dark period	CH_4 (70%), CO_2 (29.5%), H_2S (0.5%), MeSH (21.2 mg m^{-3}), Toluene (12.2 mg m^{-3}), Hexane (47.4 mg m^{-3})

* Fed during the dark period

2.2 Analytical procedures

CH_4, CO_2, H_2S, O_2 and N_2 gas concentrations were quantified using a Varian CP-3800 GC-TCD (Palo Alto, USA) equipped with a CP-Molsieve 5A (15m × 0.53mm × 15μm) and a CP-Pora BOND Q (25m × 0.53 mm × 15 μm) columns according to Posadas *et al*., [12]. Prior to the determination of MeSH, hexane and toluene concentrations, biogas samples were pre-concentrated in 500 mL glass bulbs (Altech, USA) for 1 min using 75 μm PDMS/Carboxen solid phase microextraction (SPME) fibers (Supelco, USA). The SPME fibers were injected for 1 min in a GC-FID (Agilent 4890, USA) equipped with a HP-1 column (30 m × 0.53 mm × 5 μm). Injector, detector, and oven temperatures were maintained at 300°C, 300 °C and 70°C, respectively, while Helium was used as a carrier gas at 5.2 mL min^{-1}.

IC and TN concentrations were determined using a Shimadzu TOC-VCSH analyzer (Japan) equipped with a TNM-1 chemiluminescence module. $N\text{-}NH_4^+$ was measured using an ammonia electrode Orion Dual Star (Thermo Scientific, The Netherlands), while NO_2^-,

NO_3, SO_4^{2-} and PO_4^{3-} were quantified by HPLC-IC according to Serejo *et al*., [13]. The concentration of TSS was measured according to standard methods [18]. Total phosphorus (TP) was determined spectrophotometrically using the ammonium molybdate vanadate method after sample digestion (Spectrophotometer U-2000, Hitachi, Japan). pH was measured in a Eutech Cyberscan pH 510 meter (Eutech instruments, The Netherlands), while DO concentrations were determined using an OXI 330i oximeter (WTW, Germany). Photosynthetically active radiation (PAR) was measured using a LI-250A light meter (Lincoln, Nebraska, USA).

The protein content of the algal-bacterial biomass was analyzed in a spectrophotometer U-2000 (Hitachi, Japan) according to Randall and Lewis [19]. The carbohydrate content was also determined using a colorimetric method (spectrophotometer U-2000, Hitachi, Japan) according to Dubois *et al*., [20]. Total lipids were extracted with ethyl ether for 60 min in an automatic Soxhlet extraction unit (SER 148 Series, Velp Scientifica) at an extraction temperature of 130°C. On the other hand, the carbon, nitrogen and sulfur content of the algal-bacterial biomass was quantified using a CHNS analyzer (LECO CHNS-932). The phosphorous content of the biomass was analyzed in an Inductively Coupled Plasma-Optical Emission Spectrometer (ICP-OES, Varian 725-ES) following microwave-acid digestion [14]. Finally, microalgae morphological identification was performed by microscopic observation (OLYMPUS IX70, USA) after sample fixation with 5% of lugol acid according to Sournia [21].

2.3 Statistical Analysis

Results were provided as the average and standard deviation from replicate measurements under steady-state conditions. An analysis of variance (ANOVA) was performed on the experimental data using OriginPro 8® to evaluate process performance under steady-state.

3. Results and discussion

3.1 Biogas upgrading performance

The content of CH_4 in the biomethane obtained in stages I, II and III (98.3 ± 0.9%, 97.6 ± 0.7% and 99.1 ± 1.0%, respectively) implementing biogas upgrading during the night were higher to that reported by Toledo-Cervantes *et al.*, [7] at a L/G ratio of 1 with biogas supply during the illuminated period. In addition, it complied with most international regulations for biogas injection into natural gas grids as a result of the high removal efficiencies of CO_2 and H_2S mediated by the high pH and alkalinity of the cultivation broth (Table 2) [3]. At this point, it is worth noticing that stage I served as a reference scenario in order to determine the combined effect of the trace biogas microcontaminants (i.e. MeSH, Tol, Hex) on photosynthetic biogas upgrading. In this sense, CO_2 removal efficiencies (CO_2-REs) in stage I (99.5 ± 0.2%) were significantly different (n=7, $p < 0.05$) than those achieved in stage II (97.6 ± 0.7%) likely due to the presence of VOCs and MeSH in the synthetic biogas during the latter stage (Table 2). However, CO_2-REs were not significantly different (n=6, $p > 0.05$) in stages II and III (97.6 ± 0.7% and 98.9 ± 0.4%, respectively), which confirmed that the effect of supplying digestate during the dark period was negligible. On the other hand, H_2S removal efficiencies (H_2S-REs) were not significantly affected (n=7, $p > 0.05$) by the presence of VOCs/MeSH in biogas or digestate supply during the night, with H_2S-REs of 99.3 ± 0.8%, 99.7 ± 0.7% and 100 ± 0.0%, during stages I, II and III,

229 respectively. The CO_2-REs and H_2S-REs herein recorded were similar to those reported by
230 Toledo-Cervantes *et al*., [7].

231

Table 2. Removal efficiencies of CO_2 and H_2S from biogas, and biomethane composition obtained during all operational stages

Stage	RE CO_2 (%)	RE H_2S (%)	N_2 content (%v/v)	O_2 content (%v/v)	CO_2 content (%v/v)	CH_4 content (%v/v)
I	99.5 ± 0.2	99.3 ± 0.8	1.3 ± 0.8	0.18 ± 0.17	0.2 ± 0.0	98.3 ± 0.9
II	97.6 ± 0.7	99.7 ± 0.7	0.7 ± 0.4	0.05 ± 0.05	1.8 ± 0.5	97.6 ± 0.7
III	98.9 ± 0.4	100 ± 0.0	0.6 ± 0.5	0.07 ± 0.08	0.5 ± 0.2	99.1 ± 1.0

232

233 The O_2 and N_2 content in the obtained biomethane was also in accordance with that
234 required by most European regulations during all operational stages (Table 2) [3]. The latter
235 was attributed to the interruption of photosynthetic oxygen production during the dark
236 periods concomitantly with an increase in microalgae respiration, which ultimately
237 decreased the DO concentration in the HRAP [22]. Therefore, biogas supply during the
238 dark periods minimized O_2 stripping from the cultivation broth and contribute to decreasing
239 the O_2 content in the biomethane [13]. Furthermore, the L/G ratio in this particular HRAP-
240 AC configuration which has been identified as the main operational parameter determining
241 the final quality of biomethane was optimized (L/G ratio=0.5). In this context, L/G ratios
242 lower than 1.0 minimize O_2 and N_2 stripping from the cultivation broth but entail a severe
243 acidification of the recirculating medium (that can ultimately decrease the removal
244 efficiencies of CO_2 and H_2S), unless a sufficiently high alkalinity is present in the
245 cultivation broth [23]. In addition, low L/G ratios are beneficial from an energy-reduction

viewpoint and would contribute to decreasing the overall operating cost of the photosynthetic biogas upgrading.

The MeSH, toluene, and hexane concentrations here supplemented to biogas mimicked the content of VOCs and VSCs commonly found in raw biogas [1]. The steady-state elimination capacities recorded for MeSH, toluene, and hexane were 14 ± 3 mg m^{-3} h^{-1}, 15 ± 1 mg m^{-3} h^{-1}, and 6 ± 5 mg m^{-3} h^{-1}, respectively, regardless of the digestate supply strategy. Likewise, the steady-state removal efficiencies of methyl mercaptan (MeSH-RE), hexane (Hex-RE) and toluene (Tol-RE) in stage II accounted for 59 ± 8%, 11 ± 9% and 97 ± 1%, respectively, and 66 ± 4%, 7 ± 7% and 98 ± 1%, respectively, during stage III (Figure 2). The fact that MeSH-REs, Hex-REs, and Tol-REs were not significantly different between stage II and III confirmed the negligible effect of digestate supply during the night on biogas upgrading performance. The differences in removal efficiencies encountered for the three biogas microcontaminants evaluated were attributed to their different aqueous solubilities (Henry´s law constants of toluene, MeSH and hexane of 1.5×10^{-3}, 3.32×10^{-3} and 6×10^{-6} mol m^{-3} Pa^{-1}). Nonetheless, the recorded toluene and MeSH removal efficiencies were comparable to those achieved in conventional technologies [24]. The biochemical routes involved during the process cannot be directly correlated with the biogas upgrading performance since the process was mass transfer limited. Indeed, further research focused on this topic is required but unfortunately, this was out of scope of this work.

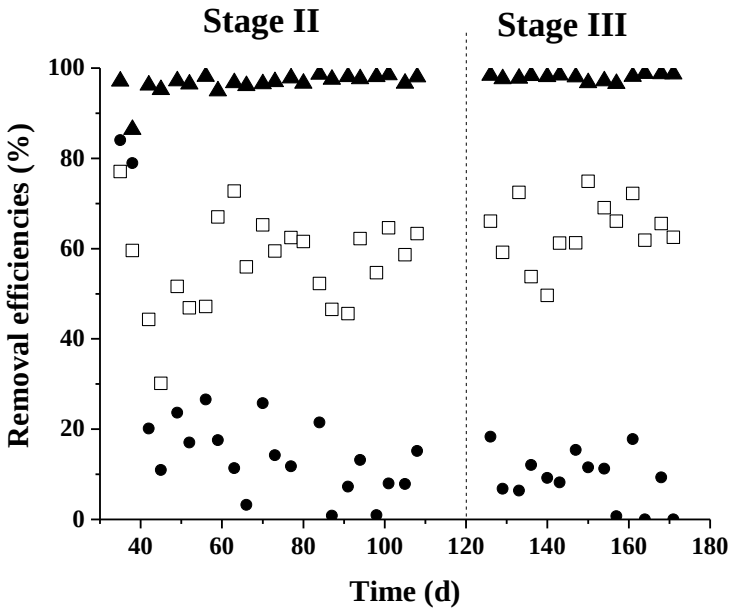

Figure 2. Time course of the removal efficiencies of methyl mercaptan (□), hexane (●) and toluene (▲) during stage II and III at hexane, toluene and MeSH inlet loading rates of 53 ± 4, 15 ± 1 and 25 ± 5 mg m^{-3} h^{-1}, respectively.

Steady-state MeSH, toluene and hexane concentrations of 13 ± 4 mg m^{-3}, 0.6 ± 0.2 mg m^{-3}, and 60 ± 6 mg m^{-3} were recorded in the biomethane (please note that a concentration of the microcontaminants occurred, as a result of the decrement in the gas volume due to CO_2 absorption). In this context, the maximum permissible concentration of MeSH in the Spanish biomethane standard is 17 mg m^{-3} and 5-10 mg m^{-3} for the standards of several EU countries [3]. In contrast, no specific regulations for hexane exist in the EU biomethane standards, while the concentration of BTX in the Dutch and Spanish standards must remain below 500 mg m^{-3}, and below 50 mg m^{-3} in the Swiss standard [4]. The biomethane standard of California (USA) is the only one with a limit in VOCs (< 0.1 pmm_v). Despite the hydrophobic nature of the target biogas microcontaminants here tested, this study confirmed the potential of photosynthetic biogas upgrading for the integral removal of VOCs and VSCs.

3.2 Digestate treatment performance

The presence of VOCs and VSCs in biogas significantly decreased ($p < 0.05$) the algal-bacterial biomass concentration in the HRAP from 1.21 ± 0.15 g L^{-1} in stage I to 0.82 ± 0.18 g L^{-1} in stage II, which might be attributed to the toxicity of the biogas microcontaminants or associated biodegradation metabolites (Table 3). A further decrease in the TSS concentration in the HRAP to 0.67 ± 0.03 g L^{-1} was recorded during stage III likely due to the supply of nutrients during the night, which might have enhanced the stripping of NH_3 and the precipitation of PO_4^{3-}. At this point, it must be highlighted that the lower steady-state TSS concentration recorded in stage II did not impact on the biomass productivity of the HRAP, which was fixed at 15 g m^{-2} d^{-1} (as described in section 2.1). However, digestate feeding during the dark period induced a severe change in the microalgae population structure (as described in section 3.3), which limited biomass separation from the cultivation broth and allowed a maximum biomass productivity of 8.3 g m^{-2} d^{-1} (Table 3).

The DO concentrations in the cultivation broth of the HRAP during the illuminated periods remained higher than 8 mg O_2 L^{-1} as a result of the intense photosynthetic activity of microalgae, regardless of the biogas or digestate feeding strategy. Nonetheless, the significant decrease in DO concentration recorded in stage II and III during the illuminated period compared to stage I might be due to the partial inhibition of photosynthetic activity mediated by the presence of VOCs and VSCs in the biogas (Table 3). In addition, the DO concentrations during the dark period decreased to values of 2.4-3.0 mg O_2 L^{-1}, which mediated the low O_2 stripping to biomethane previously discussed. On the other hand, the

pH of the cultivation remained >10 during the three operational stages, with no significant differences between the illuminated and dark periods. These high pH values supported the high CO_2-REs and H_2S-REs recorded during the entire experimental period (Table 2). Finally, the temperature of the cultivation broth slightly increased along the experimental period mediated by the seasonal increase in ambient temperature.

Table 3. Environmental and operating parameters during stages I, II and III.

Parameter	Stage I	Stage II	Stage III
TSS ($g\ L^{-1}$)	1.21 ± 0.15	0.82 ± 0.18	0.67 ± 0.03
DO light ($mg\ O_2\ L^{-1}$)	19.0 ± 1.5	11.9 ± 0.7	13.0 ± 3.4
DO dark ($mg\ O_2\ L^{-1}$)	2.5 ± 0.5	2.4 ± 0.5	3.0 ± 0.7
pH light	10.6 ± 0.2	10.1 ± 0.1	10.6 ± 0.1
pH dark	10.6 ± 0.2	10.1 ± 0.1	10.6 ± 0.1
T light (ºC)	25.8 ± 0.9	27.8 ± 2.3	29.6 ± 1.7
T dark (ºC)	21.2 ± 1.8	24.6 ± 2.3	22.3 ± 1.6
Biomass productivity ($g\ m^{-2}\ d^{-1}$)	15	15	8.3

COD removal efficiencies in the digestate under steady-state operation accounted for 93 ± 3%, 81 ± 5%, and 85 ± 4% in stages I, II and III, respectively (Figure 3), and confirmed the potential of this technology to remove organic matter from digestates. Furthermore, no significant differences in COD removal were recorded as a result of digestate supply during the dark period or biogas microcontaminants. IC removal efficiencies of ~93% were recorded in the three operational stages evaluated (Figure 3). The carbon mass balance calculations performed under steady-state operation showed that 78 ± 5%, 82 ± 4% and 43 ± 1% of the total carbon supplied to the system was assimilated in the form of algal-bacterial biomass in stages I, II and III, respectively (Table 4), while 15 ± 5%, 15 ± 4% and

323 50 ± 1% was stripped out from the HRAP during stages I, II and III, respectively. The
324 lower biomass productivity imposed by the limited biomass settling properties observed
325 during stage III caused the larger contribution of CO_2 stripping to the overall carbon
326 removal.

327

Table 4. Elemental biomass composition under steady-state in stage I, II and III.

Element	Stage I	Stage II	Stage III
Carbon (%)	43.35	41.06	40.18
Nitrogen (%)	6.95	6.59	5.74
Phosphorous (%)	0.600	0.669	0.404
Sulfur (%)	0.71	0.67	0.73

328 Expanded uncertainty (k=2)

329

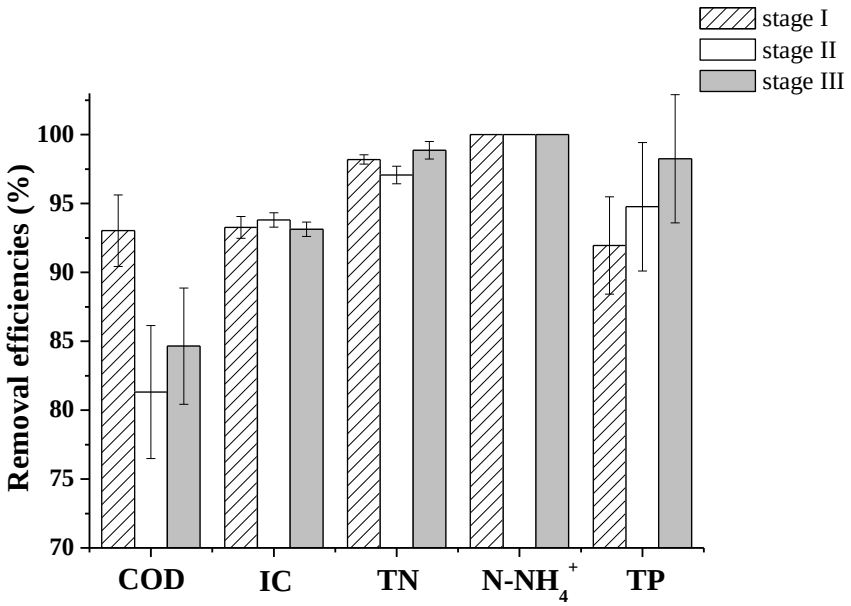

330

331 **Figure 3**. Average removal efficiencies of COD, IC, TN, N-NH_4^+, and TP. Vertical lines
332 represent the standard deviation from replicate measurements (n=6) under steady-state
333 operation.

334

The removal efficiencies of TN in the HRAP during stages I, II and III accounted for 98.2 ± 0.3%, 97.1 ± 0.6% and 98.9 ± 0.1%, respectively (Figure 3), which were in agreement with those reported by Toledo-Cervantes *et al*., [7,14] in a similar experimental set-up. Process operation in the absence of effluent (only the liquid contained in the concentrated biomass wasted from the bottom of the settler was daily drawn) supported such high nitrogen removal efficiencies. Likewise, NH_4^+ removal was complete regardless of the operational conditions tested as a result of the high rates of nitrogen assimilation, nitrification and stripping induced by the high pH prevailing in the cultivation broth (pH>10, Table 3). On the other hand, the $N\text{-}NO_3^-$ concentrations recorded under steady-state during stage I, II and III averaged 34.2 ± 14.2 mg L^{-1}, 64.71 ± 11.6 mg L^{-1}, and 3.67 ± 4.2 mg L^{-1}, respectively. The slightly higher temperature of the cultivation broth recorded during stage II likely enhanced NH_4^+ nitrification, which consequently increased NO_3^- concentrations in the cultivation broth [25]. The further seasonal increase in the temperature of the cultivation broth to 29.6 ± 1.0 °C was not capable of counterbalancing the enhanced NH_3 stripping occurred during stage III, which resulted in the low NO_3^- concentration recorded in the last operational stage. In addition, the relatively high DO concentrations prevailing in the HRAP during the dark periods (>2 mg O_2 L^{-1}) and moderate temperatures (<30ºC) likely avoided NO_2^- accumulation. Overall, the nitrogen mass balance calculations performed indicated that 87 ± 6%, 96 ± 6% and 69 ± 3% of the total nitrogen input to the HRAP was assimilated into biomass in stages I, II and III, respectively (Table 4). In this context, the TN volatilization losses estimated in stages I, II and III averaged 12 ± 6%, 2 ± 6% and 30 ± 3%, respectively, which highlights the key role of NH_3 stripping under low biomass productivity scenarios [26,27].

Unprecedentedly high steady-state phosphorous removal efficiencies were achieved in the system regardless of the biogas or digestate supply strategy (90 ± 2%, 96 ± 4% and 99 ± 1% in stage I, II and III, respectively). These TP-REs were higher than those obtained by Serejo et al., [13] and Toledo-Cervantes et al., [7] in a similar experimental set-up and were likely caused by the precipitation induced the high pH values prevailing in the cultivation broth of the HRAP (Figure 3). Similar TP-REs (91%) were recorded in a HRAP operated in a greenhouse (54 μmol m^{-2} s^{-1} of illumination) and fed with slaughterhouse wastewaters [28].

Indeed, the phosphorus mass balance calculations herein conducted showed that only 38 ± 3%, 29 ± 6% and 63 ± 2% of the total phosphorous input was assimilated into algal-bacterial biomass in stages I, II and III, respectively (Table 4). The higher removal efficiencies recorded in stage III were caused by the lower P concentrations present in the digestate during this operational stage.

All H_2S supplied to the biogas absorption column was oxidized to $S\text{-}SO_4^{2-}$ as a result of the high DO concentrations present in the HRAP during the entire experimental period (>2 mg O_2 L^{-1}) (Table 3). Indeed, DO concentrations must remain above 0.1 mg O_2 L^{-1} in order to avoid oxygen limitation during the H_2S biological oxidation [29] and prevent the formation of elemental sulfur. In our experimental set-up, $S\text{-}SO_4^{2-}$ concentrations in the digestate remained below the detection limit of the HPLC-IC, while $S\text{-}SO_4^{2-}$ concentrations averaged 67.1 ± 7.3 mg L^{-1}, 170.0 ± 9.5 mg L^{-1}, and 189.7 ± 5.1 mg L^{-1} in stages I, II and III, respectively. The sulfur mass balance calculations showed that only 40%, 36%, and 23% of the sulfur input was assimilated in the form of algal-bacterial biomass [30].

3.3 Microalgae population structure and composition

The morphological characterization of the microalgae population structure under steady-state operation revealed that the alkaline conditions present in the HRAP promoted the dominance of an unialgal culture of the green microalga *Mychonastes homosphaera (Skuja) Kalina & Puncochárová* during stage I [14]. The predominant microalga species changed to the green microalga *Chloroidium ellipsoideum* during stage II (100 % abundance) and to the cyanobacterium *Synechocystis sp*. during stage III (90 % abundance).

The morphological characterization of the microalgae population structure under steady-state operation revealed that the alkaline conditions present in the HRAP promoted the prevalence of the unialgal culture of the green microalga *Mychonastes homosphaera (Skuja) Kalina & Puncochárová* during stage I [14]. The predominant microalga species changed to the green microalga *Chloroidium ellipsoideum* during stage II (100 % abundance) and to the cyanobacterium *Synechocystis* sp. during stage III (90 % abundance). Interestingly, the modification of the nutrient feeding regime in stage III promoted the dominance of a cyanobacterium over green microalgae (dominant in stages I and II), which validated the hypothesis that microorganisms population structure can be controlled via tailored digestate supply strategies. This finding was in agreement with the recent observations of Toledo-Cervantes *et al*., [31] who reported the occurrence of a cyanobacterium during the operation of a tubular photobioreactor devoted to CO_2 abatement when digestate was fed as nutrient source during the dark period.

No significant differences were found in the protein and lipid content of the algal-bacterial biomass between the light and dark periods in stage II (Figure 4). Nonetheless, the carbohydrates content decreased from 46 ± 1% to 31 ± 2% during the dark period, which

406 suggested that these macromolecules were used as an energy reservoir for maintenance
407 purposes (endogenous respiration) in the absence of light and photosynthetically
408 synthesized during the illuminated period (Figure 4) [32,33]. During stage III, the nitrogen
409 limitation imposed by digestate feeding during the dark periods induced a decrease in the
410 protein content of the biomass from ~45% to < 30%. This decrease in the protein content
411 correlated with a decrease in the nitrogen content of the biomass from 6.9% to 5.7% (Table
412 4). On the other hand, while the carbohydrate content in biomass remained at similar levels
413 during the illuminated and dark periods of stage II and III (with only a slight decrease
414 during the dark period), the lipid content of the biomass increased >10% during stage III. In
415 this context, the rapid synthesis of sugar-based molecules in microalgae compared to fatty
416 acids synthesis could explain the fact that only carbohydrates accumulation has been
417 reported when nutrients are supplied during the night [31]. In our particular study, the
418 variation in the macromolecular composition of the biomass can be attributed to the shift in
419 microalgae population structure from the green microalga *Chloroidium ellipsoideum* to the
420 cyanobacterium *Synechocystis sp.*[34].

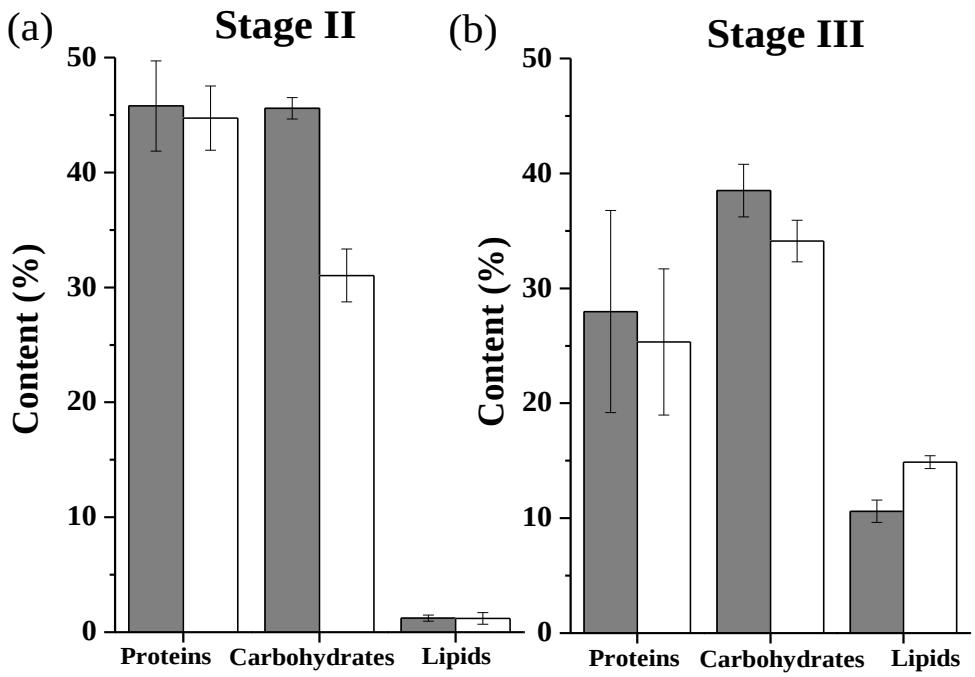

421

422 **Figure 4**. Protein, carbohydrate and lipid content in the algal-bacterial biomass at the end
423 of the illuminated period (gray bars) and dark period (white bars) during stages II (a) and
424 III (b). Vertical lines represent standard deviation from replicate measurements (n=6) under
425 steady-state operation.
426

427 ## 4. Conclusions

428 The high pH and alkalinity of the cultivation broth in the HRAP supported the generation
429 of a high-quality biomethane regardless of the biogas and digestate supply strategy. Biogas
430 supply during the dark period mediated a low content of O_2 in the biomethane (0.18-
431 0.07%) as a result of the low DO concentrations in the cultivation broth. Biomethane
432 composition was not impacted by the presence of trace levels of VOCs and VSCs in the
433 raw biogas, which were removed as a function of their aqueous solubility (Tol-REs >
434 MeSH-REs > Hex-REs). Finally, the supplementation of digestate during the dark periods
435 induced a shift in the microalgae population structure from green microalgae to

cyanobacteria, concomitantly with a decrease in the content of proteins and nitrogen, and an increase in the lipid content.

5. Acknowledgements

This research was funded by the Spanish Ministry of Economy and Competitiveness and the European Union through the FEDER Funding Program (CTM2015-70442-R and Red Novedar). The financial support from the regional government of Castilla y León is also gratefully acknowledged (UIC71). The authors thank CONACyT for the mobility grant of Mariana Franco to conduct a research stay at University of Valladolid (Spain). The financial support of the Mexican Secretary of Marine (SEMAR- Conacyt 207151) and Fondo Sectorial CONACyT-SENER, CEMIE-Bio project No. 247006 are also appreciated.

6. References

[1] N. de Arespacochaga, C. Valderrama, C. Mesa, L. Bouchy, J.L. Cortina, Biogas deep clean-up based on adsorption technologies for solid oxide fuel cell applications, Chem. Eng. J. 255 (2014) 593–603. doi:10.1016/j.cej.2014.06.072.

[2] E. Ryckebosch, M. Drouillon, H. Vervaeren, Techniques for transformation of biogas to biomethane, Biomass and Bioenergy. 35 (2011) 1633–1645. doi:10.1016/j.biombioe.2011.02.033.

[3] R. Muñoz, L. Meier, I. Diaz, D. Jeison, A review on the state-of-the-art of physical/chemical and biological technologies for biogas upgrading, Rev. Environ. Sci. Biotechnol. 14 (2015) 727–759. doi:10.1007/s11157-015-9379-1.

[4] L. Bailón Allegue, J. Hinge, Biogas and bio-syngas upgrading, 2012.

[5] M. Bahr, I. Díaz, A. Dominguez, A. González Sánchez, R. Muñoz, Microalgal-biotechnology as a platform for an integral biogas upgrading and nutrient removal from anaerobic effluents., Environ. Sci. Technol. 48 (2014) 573–81. http://www.ncbi.nlm.nih.gov/pubmed/24298934.

[6] E. Posadas, D. Marín, S. Blanco, R. Lebrero, R. Muñoz, Simultaneous biogas upgrading and centrate treatment in an outdoors pilot scale high rate algal pond, Bioresour. Technol. 232 (2017) 133–141. doi:10.1016/j.biortech.2017.01.071.

[7] A. Toledo-Cervantes, M.L. Serejo, S. Blanco, R. Pérez, R. Lebrero, R. Muñoz, Photosynthetic biogas upgrading to bio-methane: Boosting nutrient recovery via biomass productivity control, Algal Res. 17 (2016) 46–52. doi:10.1016/j.algal.2016.04.017.

[8] A. Vergara-Fernández, S. Revah, P. Moreno-Casas, F. Scott, Biofiltration of volatile organic compounds using fungi and its conceptual and mathematical modeling,

Biotechnol. Adv. 36 (2018) 1079–1093. doi:10.1016/j.biotechadv.2018.03.008.

[9] J.M. Estrada, S. Hernández, R. Muñoz, S. Revah, A comparative study of fungal and bacterial biofiltration treating a VOC mixture, J. Hazard. Mater. 250–251 (2013) 190–197. doi:10.1016/j.jhazmat.2013.01.064.

[10] X. Borde, B. Guieysse, O. Delgado, R. Muoz, R. Hatti-Kaul, C. Nugier-Chauvin, H. Patin, B. Mattiasson, Synergistic relationships in algal-bacterial microcosms for the treatment of aromatic pollutants, Bioresour. Technol. 86 (2003) 293–300. doi:10.1016/S0960-8524(02)00074-3.

[11] A. Anbalagan, A. Toledo-Cervantes, E. Posadas, E.M. Rojo, R. Lebrero, A. González-Sánchez, E. Nehrenheim, R. Muñoz, Continuous photosynthetic abatement of CO_2 and volatile organic compounds from exhaust gas coupled to wastewater treatment: Evaluation of tubular algal-bacterial photobioreactor, J. CO_2 Util. 21 (2017) 353–359. doi:10.1016/j.jcou.2017.07.016.

[12] E. Posadas, M.L. Serejo, S. Blanco, R. Pérez, P. a. García-Encina, R. Muñoz, Minimization of biomethane oxygen concentration during biogas upgrading in algal–bacterial photobioreactors, Algal Res. 12 (2015) 221–229. doi:10.1016/j.algal.2015.09.002.

[13] M.L. Serejo, E. Posadas, M.A. Boncz, S. Blanco, P. García-Encina, R. Muñoz, Influence of biogas flow rate on biomass composition during the optimization of biogas upgrading in microalgal-bacterial processes, Environ. Sci. Technol. 49 (2015) 3228–3236. doi:10.1021/es5056116.

[14] A. Toledo-Cervantes, C. Madrid-Chirinos, S. Cantera, R. Lebrero, R. Muñoz, Influence of the gas-liquid flow configuration in the absorption column on photosynthetic biogas upgrading in algal-bacterial photobioreactors, Bioresour.

Technol. 225 (2017) 336–342. doi:10.1016/j.biortech.2016.11.087.

[15] C.I. Granada-Moreno, A. Aburto-Medina, D. de los Cobos Vasconcelos, A. González-Sánchez, Microalgae community shifts during the biogas upgrading in an alkaline open photobioreactor, J. Appl. Microbiol. 123 (2017) 903–915. doi:10.1111/jam.13552.

[16] P.R. Mooij, G.R. Stouten, J. Tamis, M.C.M. van Loosdrecht, R. Kleerebezem, Survival of the fattest, Energy Environ. Sci. 6 (2013) 3404. doi:10.1039/c3ee42912a.

[17] I. de Godos, H.O. Guzman, R. Soto, P.A. García-Encina, E. Becares, R. Muñoz, V.A. Vargas, Coagulation/flocculation-based removal of algal-bacterial biomass from piggery wastewater treatment, Bioresour. Technol. 102 (2011) 923–927. doi:10.1016/j.biortech.2010.09.036.

[18] A.D. Eaton, L.S. Clesceri, A.E. Greenberg, Standard methods for the examination of water and wastewater, 21 st, Healt, Association American Public Works, Association American Water Federation, Water Environment, Washington DC, USA, 2005.

[19] R.J. Randall, A. Lewis, Protein measurement with the Folin phenol reagent, (1951).

[20] M. Dubois, K.A. Gilles, J.K. Hamilton, P.A. Rebers, F. Smith, Colorimetric method for determination of sugars and related substances, Anal. Chem. 28 (1956) 350–356.

[21] A. Sournia, Phytoplankton Manual, UNESCO, Paris, 1978. doi:10.2216/i0031-8884-19-4-341.1.

[22] D. Kaplan, A. Richmond, Algal nutrition, in: R. Amos (Ed.), Handb., Blackwell Publishing, UK, 1986: pp. 95--115. https://scholar.google.com.mx/scholar?q=kaplan+1986+Algal+nutrition&btnG=&hl=es&as_sdt=0%2C5.

[23] R. Rodero, Posadas, E., Toledo-Cervantes, A., Lebrero, R., Muñoz, Influence of

520 alkalinity and temperature on photosynthetic biogas upgrading efficiency in high rate
521 algal ponds, Algal Res. 33 (2017) 284–290. doi:10.1016/j.algal.2018.06.001.
522 [24] R. Iranpour, H.H.J. Cox, M.A. Deshusses, E.D. Schroeder, Literature review of air
523 pollution control biofilters and biotrickling filters for odor and volatile organic
524 compound removal, Environ. Prog. 24 (2005) 254–267. doi:10.1002/ep.10077.
525 [25] D.J. Kim, D.I. Lee, J. Keller, Effect of temperature and free ammonia on nitrification
526 and nitrite accumulation in landfill leachate and analysis of its nitrifying bacterial
527 community by FISH, Bioresour. Technol. 97 (2006) 459–468.
528 doi:10.1016/j.biortech.2005.03.032.
529 [26] Y. Peng, G. Zhu, Biological nitrogen removal with nitrification and denitrification
530 via nitrite pathway, Appl. Microbiol. Biotechnol. 73 (2006) 15–26.
531 doi:10.1007/s00253-006-0534-z.
532 [27] J. Wang, Y. Peng, S. Wang, Y. Gao, Nitrogen removal by simultaneous nitrification
533 and denitrification via nitrite in a sequence hybrid biological reactor, Chinese J.
534 Chem. Eng. 16 (2008) 778–784. doi:10.1016/S1004-9541(08)60155-X.
535 [28] D. Hernández, B. Riaño, M. Coca, M. Solana, A. Bertucco, M.C. García-González,
536 Microalgae cultivation in high rate algal ponds using slaughterhouse wastewater for
537 biofuel applications, Chem. Eng. J. 285 (2016) 449–458.
538 doi:10.1016/j.cej.2015.09.072.
539 [29] A.J.H. Janssen, R. Sleyster, C. Van der Kaa, A. Jochemsen, J. Bontsema, G.
540 Lettinga, Biological sulphide oxidation in a fed-batch reactor, Biotechnol. Bioeng.
541 47 (1995) 327–333. doi:10.1002/bit.260470307.
542 [30] A. González-Sánchez, C. Posten, Fate of H_2S during the cultivation of *Chlorella sp*.
543 deployed for biogas upgrading, J. Environ. Manage. 191 (2017) 252–257.

544 doi:10.1016/j.jenvman.2017.01.023.
545 [31] A. Toledo-cervantes, T. Morales, Á. González, R. Muñoz, R. Lebrero, Long-term
546 photosynthetic CO_2 removal from biogas and fl ue-gas : exploring the potential of
547 closed photobioreactors for high-value biomass production, Sci. Total Environ. 640–
548 641 (2018) 1272–1278. doi:10.1016/j.scitotenv.2018.05.270.
549 [32] G. Markou, D. Vandamme, K. Muylaert, Microalgal and cyanobacterial cultivation:
550 The supply of nutrients, Water Res. 65 (2014) 186–202.
551 doi:10.1016/j.watres.2014.07.025.
552 [33] M. Franco-Morgado, C. Alcántara, A. Noyola, R. Muñoz, A. González-Sánchez, A
553 study of photosynthetic biogas upgrading based on a high rate algal pond under
554 alkaline conditions: Influence of the illumination regime, Sci. Total Environ. 592
555 (2017) 419–425. doi:10.1016/j.scitotenv.2017.03.077.
556 [34] B. Xie, W. Gong, Y. Tian, F. Qu, Y. Luo, X. Du, X. Tang, D. Xu, DachaoLin, G. Li,
557 H. Liang, Biodiesel production with the simultaneous removal of nitrogen,
558 phosphorus and COD in microalgal-bacterial communities for the treatment of
559 anaerobic digestion effluent in photobioreactors, Chem. Eng. J. 350 (2018) 1092–
560 1102. doi:10.1016/J.CEJ.2018.06.032.
561
562

Table 1

Table 1. Operational conditions evaluated in the experimental HRAP-AC system

Stage	Digestate feeding	Synthetic biogas composition*
I	Illuminated period	CH_4 (70%), CO_2 (29.5%) and H_2S (0.5%)
II	Illuminated period	CH_4 (70%), CO_2 (29.5%), H_2S (0.5%), MeSH (21.2 mg m^{-3}), Toluene (12.2 mg m^{-3}), Hexane (47.4 mg m^{-3})
III	Dark period	CH_4 (70%), CO_2 (29.5%), H_2S (0.5%), MeSH (21.2 mg m^{-3}), Toluene (12.2 mg m^{-3}), Hexane (47.4 mg m^{-3})

* Fed during the dark period

Table 2

Table 2. Removal efficiencies of CO_2 and H_2S from biogas, and biomethane composition obtained during all operational stages

Stage	RE CO_2 (%)	RE H_2S (%)	N_2 content (%v/v)	O_2 content (%v/v)	CO_2 content (%v/v)	CH_4 content (%v/v)
I	99.5 ± 0.2	99.3 ± 0.8	1.3 ± 0.8	0.18 ± 0.17	0.2 ± 0.0	98.3 ± 0.9
II	97.6 ± 0.7	99.7 ± 0.7	0.7 ± 0.4	0.05 ± 0.05	1.8 ± 0.5	97.6 ± 0.7
III	98.9 ± 0.4	100 ± 0.0	0.6 ± 0.5	0.07 ± 0.08	0.5 ± 0.2	99.1 ± 1.0

Table 3

Table 3. Environmental and operating parameters during stages I, II and III.

Parameter	Stage I	Stage II	Stage III
TSS (g L^{-1})	1.21 ± 0.15	0.82 ± 0.18	0.67 ± 0.03
DO light (mg O_2 L^{-1})	19.0 ± 1.5	11.9 ± 0.7	13.0 ± 3.4
DO dark (mg O_2 L^{-1})	2.5 ± 0.5	2.4 ± 0.5	3.0 ± 0.7
pH light	10.6 ± 0.2	10.1 ± 0.1	10.6 ± 0.1
pH dark	10.6 ± 0.2	10.1 ± 0.1	10.6 ± 0.1
T light (ºC)	25.8 ± 0.9	27.8 ± 2.3	29.6 ± 1.7
T dark (ºC)	21.2 ± 1.8	24.6 ± 2.3	22.3 ± 1.6
Biomass productivity (g m^{-2} d^{-1})	15	15	8.3

Table 4

Table 4. Elemental biomass composition under steady-state in stage I, II and III.

Element	Stage I	Stage II	Stage III
Carbon (%)	43.35	41.06	40.18
Nitrogen (%)	6.95	6.59	5.74
Phosphorous (%)	0.600	0.669	0.404
Sulfur (%)	0.71	0.67	0.73

Expanded uncertainty (k=2)

Figure 1
Click here to download high resolution image

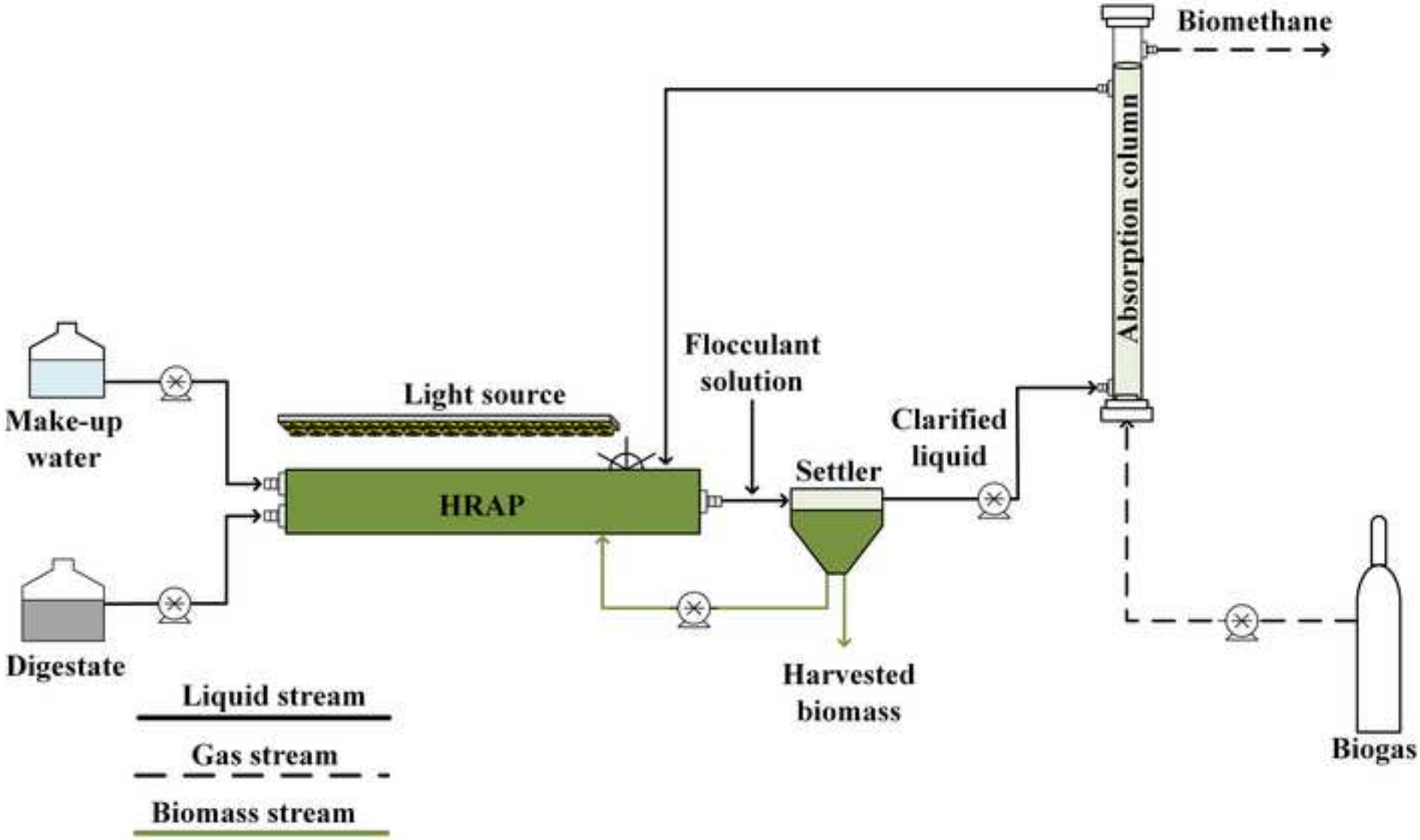

Figure 2

Click here to download high resolution image

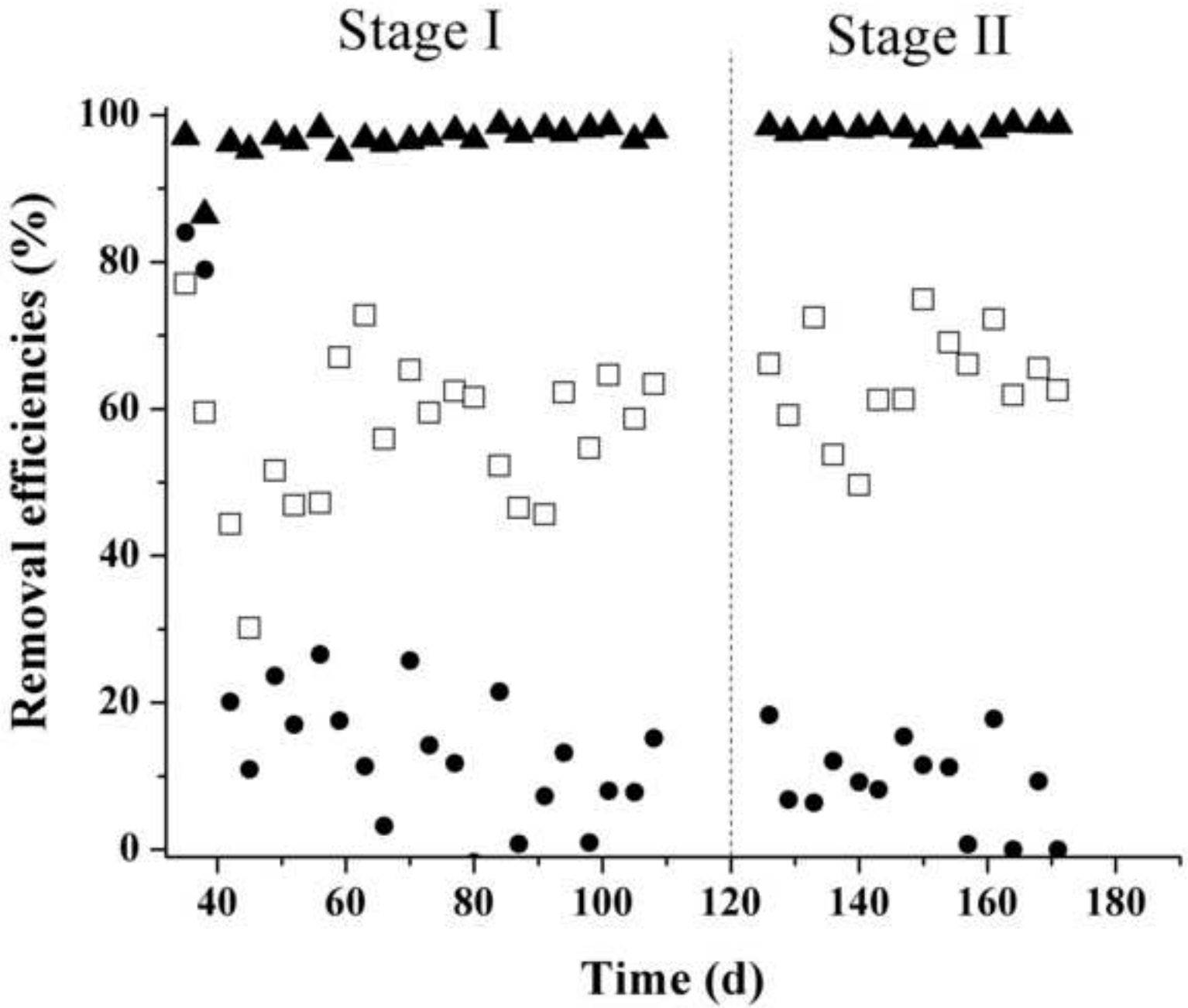

Figure 3

Click here to download high resolution image

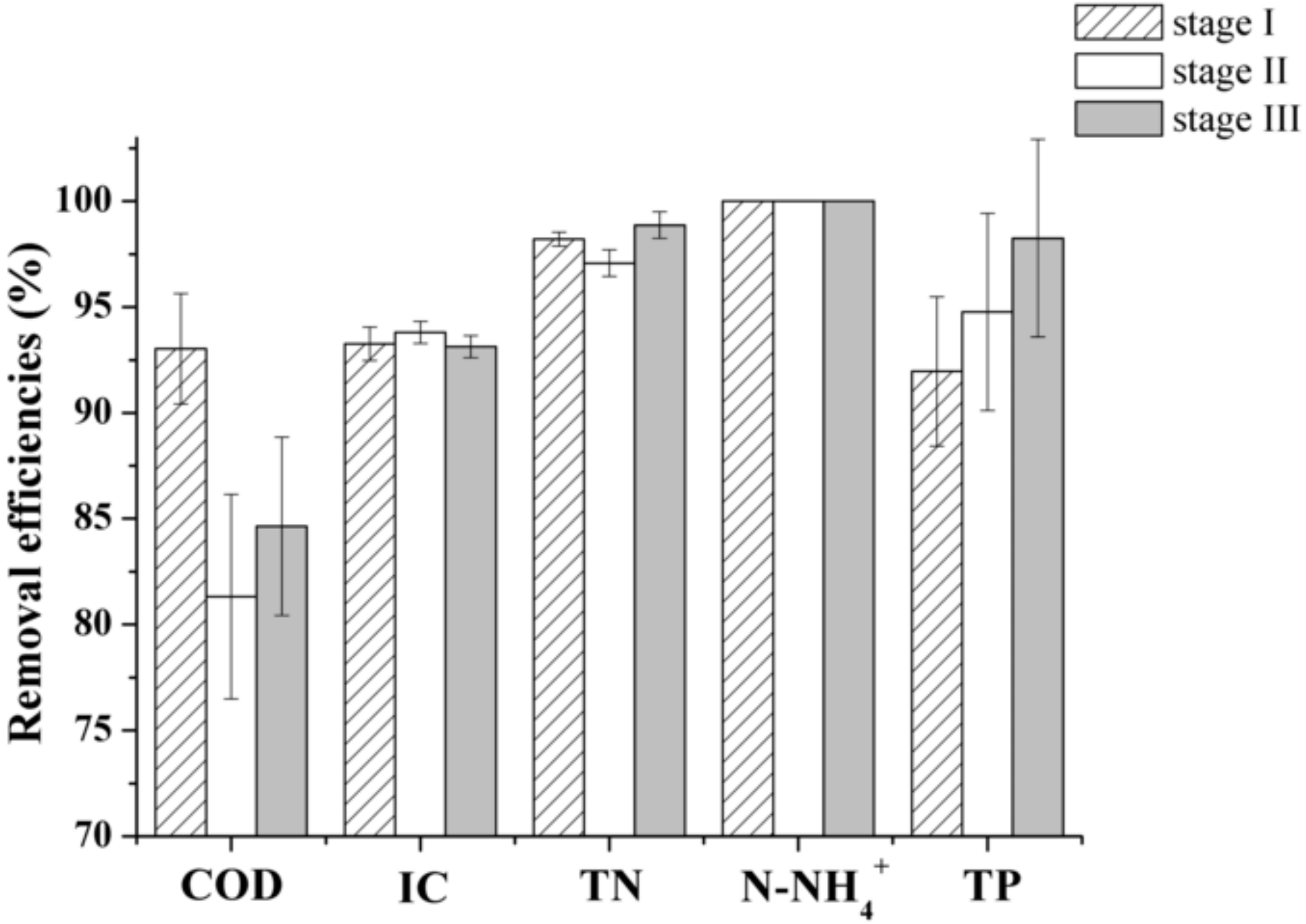

Figure 4

Click here to download high resolution image